Impulse Radio-Ultra Wideband Communications for Localisation and Tracking of Human Body and Limbs Movement for Healthcare Applications

Richa Bharadwaj, *Member IEEE*, Srijittra Swaisaenyakorn, *Member IEEE*, Clive G. Parini, *Member, IEEE,* John C. Batchelor, *Senior Member, IEEE* and Akram Alomainy, *Senior Member, IEEE*

Abstract—Accurate and precise motion tracking of limbs and human subjects has technological importance in various healthcare applications. The use of Impulse Radio Ultra Wideband (UWB) technology due its inherent properties is of recent interest for high accuracy localisation. This paper presents experimental investigations and analysis of indoor human body localisation and tracking of limb movements in 3D based on IR-UWB technology using compact and cost-effective body worn antennas. The body–centric wireless channel characterisation has been analysed in detail using parameters such as path loss magnitude, number of multipath components, RMS delay spread, signal amplitude and Kurtosis with the main focus to differentiate between line-of-sight (LOS) and non-line-of-sight (NLOS) situations. Fidelity of the received signal is also calculated for different activities and antenna positions to study the pulse preserving nature of the UWB antenna when it is placed on the human body. The results reported in this paper have high localisation accuracy with 90 % in the range of 0.5 to 2.5 cm using simple and cost-effective techniques which is comparable to the results obtained by the standard optical motion capture system.

Index Terms— **Body-worn antenna, healthcare, localisation, time of arrival, tracking, ultra wideband technology**

I. INTRODUCTION

In recent years, the localisation and tracking of static and dynamic targets has received significant interest for several upcoming applications in wireless body sensor networks. In particular, wearable wireless systems are attracting significant interest to access and monitor human activity for sports, healthcare, military applications and day-to-day activities [1-4]. These include various technologies such as as infrared, inertial, ultrasound, optical and Radio Frequency (RF) based systems [4-5]. Infrared (IR) signals are low power and inexpensive but they cannot penetrate through obstructions. The systems based on ultrasound technology are relatively cheap; however they have lower precision in comparison with IR systems and are suitable for short range only [5-8]. A problem with inertial sensors such as accelerometers is that they suffer from a

R. Bharadwaj was with the School of Electronic Engineering and Computer Science, Queen Mary University of London, London, U.K and is now with the Centre for Applied Research in Electronics, Indian Institute of Technology Delhi, New Delhi 110016, India. (email: richa_b.cstaff@care.iitd.ac.in)
C. G. Parini, and A. Alomainy are with the School of Electronic Engineering and Computer Science, Queen Mary University of London, London E1 4NS, U.K. (e-mail: a.alomainy@qmul.ac.uk).
S. Swaisaenyakorn and J.C. Batchelor are with the University of Kent, Canterbury CT2 7NT, U.K.

fluctuating offset and complex calibration procedure [9] while optical-based motion capture systems provide high accuracy but are expensive, require long calibration procedures, suffer from occlusions and are mostly confined to lab based measurements.

Among radio frequency (RF) technologies, the ultra-short pulse UWB (3.1 to 10.6 GHz) based systems enables high localisation accuracy and have several advantages such as low cost, low power, high data rate, portability, integration with other technologies (such as MEMS, inertial) and can carry signals through many obstacles in comparison to narrowband systems [10-12]. Commercial UWB localisation systems have reported an accuracy of $10 - 15$ cm with an operating range of around 50 m [12]. 3D motion tracking products based upon miniature (MEMS) inertial sensors and UWB technology enables 5-8 cm positioning accuracy in an area of 20×20 m^2 [13]. High accuracy in the range of 1 to 5 cm has been reported in the open literature for short-range indoor UWB positioning systems [12-17] and in [12], sub-millimetre accuracy is achieved using a carrier based UWB localisation system. Thus UWB technology has widespread advantages in positioning systems making it a natural choice for localisation using body worn antennas.

In [18], time of arrival (TOA) estimation using IR-UWB devices mainly for on-body arm tracking through Round Trip-Time-Of-Flight (RT-TOF) is presented obtaining an accuracy of 20 cm. TOA ranging error for indoor human tracking applications is investigated in [19] for different bandwidths ranging from 500 MHz to 5 GHz with ranging accuracy varying from several metres for low bandwidth to 0.19 m. Hybrid motion tracking system based on inertial motion capture and commercial UWB system and Kalman filter fusion algorithm is studied in [20] showing an improvement in range accuracy from 0.56 cm to 0.14 cm using UWB technology for global localisation estimation. Higher theoretical accuracy has been achieved using additional system hardware [21] in LOS situation for ankle-to-ankle distance during gait analysis, capable of providing a ranging accuracy of 0.11 cm error.

In our previous work [16-17] we studied the localisation of body worn antennas on the upper body of a human subject in uncluttered and realistic indoor environments. The promising high accuracy results (1 to 3 cm accuracy) of this investigation motivated a further detailed study in terms of motion tracking of the upper and lower limbs with whole body localisation focused for healthcare applications such as clinical motion analysis, physiotherapy and rehabilitation.

In this paper, indoor localisation of human body and tracking of limb movements is studied and analysed using wearable compact UWB antennas placed on different locations/joints of the body. UWB channel characterisation is studied in detail for various activities and the information obtained is used to minimise the error obtained in the range and localisation results, hence enabling accurate localisation and motion tracking of the wearable nodes. To the best of the authors' knowledge, very limited work is presented in the open literature in the field of limb movement localisation of human subjects using UWB technology.

The main objective of the work is to accurately determine and track a person's position and motion activity in an indoor environment using UWB channel characterisation information and time of arrival positioning techniques. The rest of the paper is organized as follows. The localisation measurement set up and scenarios are presented in section II. Section III and IV briefly describes the localisation techniques applied and detailed channel characterisation for the various activities considered related to path loss analysis, multipath and NLOS scenarios, RMS delay spread, and Kurtosis for different antenna locations and body worn antenna orientation. The results and findings are discussed in section V. Finally, concluding remarks are drawn in Section VI.

II. MEASUREMENT SET-UP

Measurements were performed in the motion capture studio at the University of Kent, UK [16, 22]. A human test subject 1.68 m tall and of average male build with a BMI of 21.3 was chosen for localising antennas on the body (Fig. 1 (a)). The antenna locations chosen for limb movement analysis are the three joints, (shoulder, elbow and wrist) for the arm and (thigh, knee and ankle) for the leg. The arm movement was measured in nine different positions ($0°$, $15°$, $30°$, $45°$, $60°$, $75°$, $90°$, $105°$, $120°$) with intervals of $15°$ forward and sideways. The leg was moved in six different positions ($-30°$, $-15°$, $0°$, $+15°$, $+30°$, $+45°$) in total (forward and backward) by $15°$ intervals during the motion capture measurements. A digital protractor was used to measure the angles with respect to the shoulder/thigh joint which is considered as reference for the arm/leg movement. The localisation of the whole body is performed using 21 antenna positions placed on the (arms and legs) limbs and torso when the subject is standing at the centre of the localisation area. For upper limb forward movement, rotation axis is the x axis and motion is taking place in y-z plane for upper limb forward movement. For the upper limb movement sideways motion, rotation axis is the y-axis and motion is taking place in x-z plane. For the lower limb forward and backward movement rotation axis is the x-axis (motion taking place in y-z plane).

The four base stations (BS) with BS1 as reference zero co-ordinate (x_0, y_0, z_0) are positioned near the vertices of the cuboid in an area of 1.8×1.8 m^2 to obtain high accuracy positioning in three dimensions [23].

Compact and low cost tapered slot co-planar waveguide fed UWB antennas (TSA) (Fig. 1 (b), [24]) were used as transmitters placed on the body and also as receivers in the base stations [16]. The TSA antenna has dimensions of 27 mm $\times$ 16 mm and offers a return loss below -10 dB with good radiation performance and relatively constant gain across the UWB band when off, or on a human body [16].
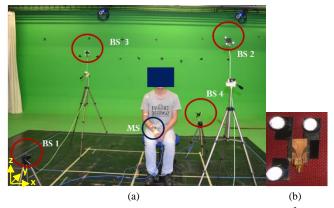

(a)   (b)

Fig. 1. (a) Measurement set up and venue in an area of 1.8 x 1.8 m^2. The base stations (red circles) and the body worn antenna (blue circle) were connected to a four-port vector network analyser. (b) Tapered Slot UWB antenna placed on a plastic frame with reflective markers.

The antennas were mounted on plastic frames with 3 reflective markers on each (Fig. 1) to provide benchmark 3D position information through a VICON motion capture system [16]. The 8 cameras motion capture system which gives high accuracy results (better than 1 cm) was used to compare with the UWB localisation results and also to obtain reference coordinates of the base stations (receiver antennas).

Frequency domain measurements were performed in the 3 to 10 GHz band using a 4-port vector network analyzer (VNA R&S ZVA-50) to capture S_{21} (channel transfer function) parameters between each transmitter antenna location on the body and the BS (receiver) antenna. For each BS and mobile station (MS) antenna position, the channel impulse response was obtained from the S_{21} collected from the VNA set to 6400 data samples, which is adequate to obtain the required channel information. For the case of limb movement tracking, measurements were taken for each of the wearable antenna location and the data is further combined together to get the overall limb localisation in three dimensions. The subject is made to hold to a particular position before proceeding to the next position with the VNA scanning time of around 800 msec to mimic the limb motion, hence obtaining a pseudo-dynamic motion for the limbs. For the case of the whole body, the antenna is positioned at different locations and readings are taken from the VNA.

III. BODY-WORN ANTENNA LOCALISATION TECHNIQUES

The time of arrival (TOA) positioning techniques are used due to the fine time resolution/high bandwidth of the UWB signal [23-25]. Figure 2 shows the proposed localisation algorithm [16] for dealing with multipath and non-line of sight NLOS situations mainly developed for human body localisation and limb movement tracking. The algorithm is based on Channel Impulse Response (CIR) characterisation and time of arrival peak detection and data fusion techniques [16-17, 26-29]. Firstly, the CIR and the received signal are obtained between each MS and BS pair. In order to obtain the CIR, an Inverse Fast Fourier Transform (IFFT) is applied to the measured S_{21}. The CIR is given by [27]:

$$h(\tau, t) = \sum_{k=1}^{K} a_k(t)\delta(\tau - \tau_k)e^{j\theta_k(t)} \qquad (1)$$

where δ is the Dirac delta function, K is the number of resolvable multipath components, τ_k are the delays of the multipath components, a_k are the path amplitude values and θ_k are the path phase values.

As shown in Fig. 2, first total line of sight (LOS) links are distinguished (with more than 95 % accuracy) from the non-line of sight (NLOS) or partial NLOS using the measured channel data obtained for each MS-BS link. The values obtained for each channel parameter is compared with the predefined parameter threshold values. The thresholds have been chosen by considering prior statistical information regarding the channel behaviour through initial measurement data. If the channel parameter value is lesser or equal to the predefined parameter values such as path loss, (PL$_{LOS}$); RMS delay spread, ($\tau_{rms(LOS)}$); multipath components, (MPC$_{LOS}$); and greater than the CIR parameter values: received signal amplitude, (A$_{LOS}$) and Kurtosis, (κ_{LOS}); LOS scenario is identified. The thresholds chosen have been optimised for the particular scenario and will vary with the change in environment. For example, for the current measurements, PL values in the range of 50 to 60 dB are considered as total LOS situation, RMS delay spread values lower than 5 nsec at -20 dB threshold of the power delay profile (PDP), and CIR having Kurtosis values higher than 45 is considered as LOS situation which are based on the maximum dimensions within the measurement area and understanding of the environment. Detailed analysis of each parameter with respect to the wearable antenna location and BS position is given in the next section.

Once, total LOS scenarios are distinguished, the remaining NLOS or partial NLOS/LOS links, are further classified with 95 % accuracy using two parameters: RMS delay spread and Kurtosis . The RMS Delay spread is defined as:

$$\tau_{rms} = \sqrt{\frac{\sum_k (\tau_k - \tau_m)^2 \cdot |h(\tau_k; d)|^2}{\sum_k |h(\tau_k; d)|^2}} \qquad (2)$$

where τ_k are the multipath delays relative to the first arriving multipath component and d is the separating distance between the Tx and Rx. This parameter helps to distinguish between LOS and NLOS links as the RMS values for NLOS scenarios are much larger.

Due the dense multipath components, NLOS CIR has a wider distribution in comparison to LOS, which has a clearly distinguishable maximum peak with multipath components of very low magnitude. The Kurtosis is a statistical parameter that indicates the fourth order moment of the received signal amplitude [30-32]. Kurtosis κ is defined as follows:

$$\kappa(x) = \frac{1}{\sigma^4} \frac{\sum_i (x_i - \bar{x})^4}{N} \qquad (3)$$

where σ is the standard deviation of the variable x and $\bar{x}$ is the mean value of x. N is the number of samples of x. The Kurtosis index κ is supposed to be much lower for NLOS scenarios in comparison to LOS.

RMS delay spread values higher than predefined $\tau_{rms(NLOS)}$ (e.g. 8 nsec) and Kurtosis values lower than κ_{NLOS} (e.g. 25) are considered as NLOS situations. Intermediate values between (5-8 nsec $\tau_{rms(PNLOS)}$ and 25-45 κ_{PNLOS}) help to further classify NLOS and partial NLOS/LOS situations. The maximum peak

detection algorithm provides an estimate of the time of arrival of the UWB signal between Tx and Rx for line-of-sight (LOS) situations [31]. The strongest peak of the CIR is considered an estimate of TOA and gives accurate results for scenarios with low multipath components and interference levels.
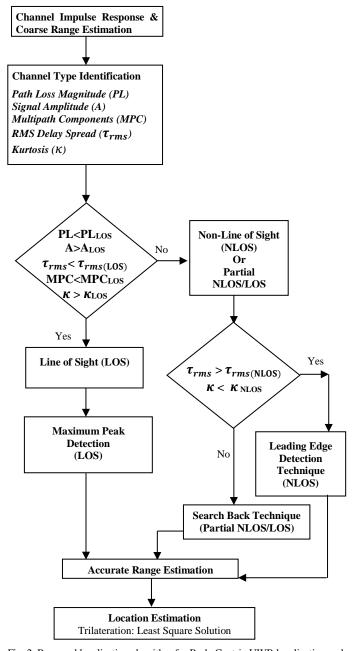

Fig. 2. Proposed localisation algorithm for Body Centric UWB localization and motion tracking applications.

In NLOS situations, the direct signal between Tx and Rx is significantly attenuated due to presence of obstructions. The strongest path in such scenarios does not give the direct path estimate, leading to large ranging errors. In addition, the human body acts like an obstacle, hence causing NLOS and high multipath situations. In order to mitigate NLOS errors and accurately estimate the range, threshold based algorithms are used [32-33]. Threshold-based search algorithms [34] compare individual signal samples with a certain threshold in order to identify the first arriving signal and obtain the range

information [35]. For total NLOS scenarios, threshold based leading edge detection algorithms can be used with selected threshold generally around 10-20 % of the peak CIR amplitude depending on the magnitude of the CIR peaks prior to the peak value. Search back technique can be used to estimate the range for partial LOS/NLOS scenarios that fall under the intermediate channel classification parameter values. The search back method first finds the strongest path (SP), and then looks for a peak arriving before the strongest path, which has greater power than a detection threshold level. A few iterations are required in order to obtain the peak value nearest the expected one or within the localisation range based on the selected threshold level.

After acquiring accurate range estimates for each MS-BS link, TOA-based mobile location algorithm is applied based on trilateration and least square solution in order to determine the unknown position of the antenna [36-37]. The distances r_1, r_2, r_3 and r_4 are used to estimate the position of the target (x_s, y_s, z_s) by solving the following set of equations using least square solution [38]:

$$r_i^2 = (x_i - x_s)^2 + (y_i - y_s)^2 + (z_i - z_s)^2 \qquad (4)$$

where i =1,2,3,4 and r_i represents the range measurements obtained from the distance between the MS and BS.

IV. CHANNEL PARAMETERS ANALYSIS

A. Path loss analysis

One of the most important aspects of statistical characterisation is describing the fluctuations of the received signal with respect to the distance. The path loss model signifies the local average received signal power (P_r) relative to the transmit power (P_t) [39-40] and is directly calculated from the measured data by averaging the measured frequency transfers at each frequency point [39-41].

Limbs Motion Tracking: The path loss magnitude for various positions of the arm is shown in Fig. 3 with respect to BS1 and BS4 during sideways arm movement activity. Figure 3(a) clearly shows the increase in path loss for the body worn antennas placed on the wrist as the arm moves from 0° to 120°. The variation in PL is maximum for the wrist (e.g. BS1: 55 to 70 dB) and ankle (e.g. BS2: 60 to 70 dB) as larger displacement is taking place during limb motion in comparison to the elbow/shoulder and knee/thigh location respectively. Over all for BS1 more links are in LOS situation having lower path loss magnitude and for BS4 NLOS situation is observed with higher magnitude of path loss leading to more attenuation. For BS2 and BS3, the magnitude of PL is high (e.g. for BS3: 70 dB) for 0° position and decreases as the arm moves to 120° position (e.g. for BS3: 55 dB) as the distance will reduce between the BS and MS. Similarly the magnitude of PL is more for BS2 right leg motion for -30° in comparison to + 45°and vice versa for BS3-MS link.

Human Body Localisation: The path loss magnitude for BS1-BS4 for various antenna nodes location on the body is shown in Fig. 4. From the graph, it can be observed that BS1,3 and BS1,2 have lower magnitude of PL as LOS links are formed for right limbs (S1-S6) and torso region (S16-S18) respectively. The overall variation in PL values obtained with respect to BS1 and

BS4 is shown in Fig. 5. It is observed that, for BS1, the right limbs and torso have a PL magnitude ranging from 50 to 55 dB
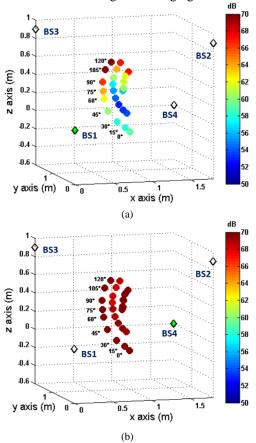

(a)

(b)

Fig. 3. Path loss magnitude colour graph for various wearable node positions (S1-S3) with respect to different base station location (a) BS1 and (b) BS4 for sideways right arm movement.
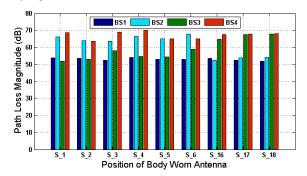

Fig. 4. Variation of the path loss magnitude with respect to the base stations (BS1-BS4) and the wearable antenna. Antenna positions: S1-S3; S4-S6; S16-S18 (Right arm, Right leg, Torso centre).

whereas the left limbs have PL from 63 to 70 dB. The PL magnitude for the left shoulder is highest for BS1 case as it is at maximum distance from BS1 showing distance dependency. For BS4 higher magnitude of path loss is obtained for right limbs and torso in comparison to the left limbs. Hence more attenuation of the received signal is observed for the NLOS situations. From the measured data it can be concluded that path loss magnitude generally in the range of 50-60 depicts LOS situations and for 60 to 70 NLOS situations occur.
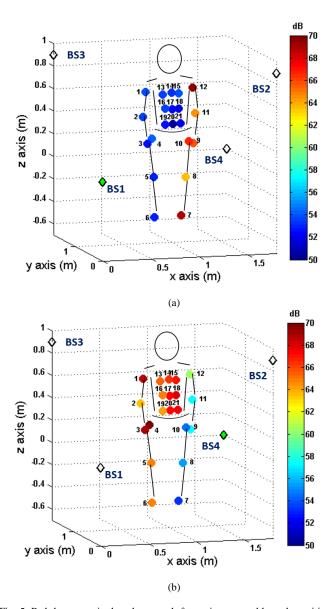
(a)

(b)

Fig. 5. Path loss magnitude colour graph for various wearable node positions (S1-S21) with respect to different base station locations (a) BS1 and (b) BS4 for the human body localisation.

B. Amplitude of Received Signal

Different levels of magnitude are observed for each wearable antenna position that is dependent on the distance between the MS-BS link, the channel type i.e. (LOS or NLOS) and orientation of the antenna with respect to each other.
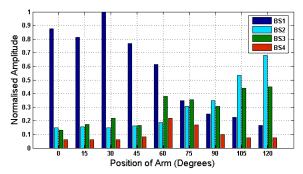

Fig. 6. Variation of amplitude of the received signal with respect to different base stations when the antenna is placed on the right wrist (S1).

Limbs Motion Tracking: BS1 is generally in LOS situation for nearly all antenna positions with highest signal amplitude in comparison to BS4, which is in NLOS situation due to shadowing by the human subject. Figure 6 demonstrates the variation in normalised amplitude value for the forward wrist motion. For BS1, the signal magnitude decreases from 30 to 120 degrees as MS-BS distance is increasing. It can be observed that the magnitude is generally lower for 0 to $60°$ orientations and then rises from 75 to 120 degrees for BS2 and BS3. There is a drastic reduction in magnitude for BS4 as it is in NLOS situation with maximum percentage decrease as high as 90 % of the magnitude level of BS1. Substantial amplitude variations are observed for antennas placed on the wrist/ankle due to higher displacements of positions caused by the arm/leg movements.

Human Body Localisation: The amplitude of the received signal is higher for BS2-left elbow and shoulder link as there is least distance between the BS and the antennas and is also in direct LOS situation. Lowest values of amplitude are observed for BS4 when the antenna is placed on the torso region in comparison to BS1. Lower values are observed for BS3,4 as they are generally in NLOS situation leading to distortion of the signal. The human subject is facing BS1 and BS2, hence high levels of signal amplitude is observed. Figure 7 shows the variation in signal amplitude for wearable antenna locations with respect to different base stations.
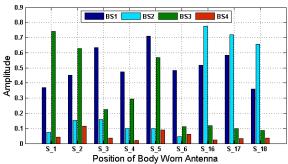

Fig. 7. Variation of the amplitude of the received signal with respect to the base stations (BS1-BS4) and the wearable antenna. Antenna positions: S1-S3; S4-S6; S16-S18 (Right arm, Right leg, Torso centre).

MS-BS distance and Peak Signal Amplitude: Knowledge of the magnitude of the received signals, gives an indication of which antennas are in LOS or NLOS situation and also an idea of the distance between Tx and Rx. Considering the highest signal amplitude among the measured data as reference, the signals are normalized with respect to the reference signal. For values above 30 % of the highest signal amplitude LOS situations are present and for below 20-30 % of the highest signal amplitude more chances of NLOS situations are present.

For wrist motion, BS1,2,3 are generally in LOS situation showing linear dependence with distance and BS4 in NLOS which can be clearly depicted in the Fig. 8 (a). In Fig. 8 (b), two large clusters can be observed of high and low amplitude at approximately 0.3 normalised signal amplitude for whole body localisation. In Fig. 8 (a) only one wearable antenna location is considered positioning itself at different angles, hence the trend is more distinct in comparison to Fig. 8 (b) where different wearable antenna locations are considered. This phenomenon is very complex, as there are several parameters that effect the received signal amplitude, it is more justified to say for LOS

This article has been accepted for publication in a future issue of this journal, but has not been fully edited. Content may change prior to final publication. Citation information: DOI 10.1109/TAP.2017.2759841, IEEE Transactions on Antennas and Propagation

> REPLACE THIS LINE WITH YOUR PAPER IDENTIFICATION NUMBER (DOUBLE-CLICK HERE TO EDIT) <   6

situations that the signal strength decreases linearly with MS-BS distance. As for NLOS the type of obstacle (physical dimensions, material) causing obstruction will make a huge difference in signal amplitude leading to non-linear relationship.
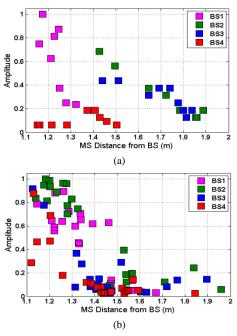

Fig. 8. Relationship between amplitude of the received signal and MS-BS distance for different base stations and wearable antenna body locations (a) wrist motion and (b) whole body localisation.

For the wrist movement, the correlation coefficient considering a linear relationship is 0.8, 0.98, 0.85, 0.5 for BS1, BS2, BS3 and BS4 respectively. For whole body localisation, the correlation coefficient considering a linear relationship is 0.88, 0.85, 0.60, 0.75 for BS1, BS2, BS3 and BS4 respectively. The received signal amplitude does not seem to decrease purely as a function of MS-BS distance but also depends on the base station location. For instance as shown in Fig. 8 (b) the exponential decay with respect to distance seems more evident for BS3 and BS4 (more NLOS links) than for BS1 and BS2 (more LOS links) which shows more linear trend.

C. Number of Multipath Components

Number of multipath components (MPC) are computed for different thresholds levels (-10, -20 and -30 dB) of the normalised power delay profile (PDP). Figure 9 (a) and (b) presents LOS and NLOS scenario of the PDP respectively. Table I. and II. presents the results for various BSs and wearable antenna links. Total NLOS links are highlighted in red.

Limbs Motion Tracking: As seen in Table I., for sideways limb motion BS1 and BS3 mostly form LOS links and have similar number of multipath components. For BS2, there is an increase in number of MPCs in comparison to BS1 and BS3. For the forward limb motion of the right arm less MPC's are present for BS1,2 in comparison to BS3. As seen from Table I., the leg motion results also have a similar trend with BS1,3. BS2 is in NLOS situation and show higher range of MPC's in comparison to the values for the arm movement. For BS4 maximum MPC's are observed for all the cases for the right limb movement due to occurrence of NLOS links. For LOS situations the

percentage increase in MPCs is generally more in comparison to NLOS situations with decrease in PDP threshold. Highest number of MPCs are observed for the shoulder and thigh region as they are totally obstructed due to the torso of the body.
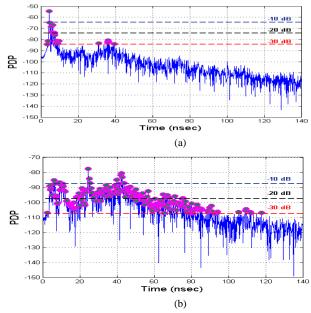

Fig. 9. Number of multipath components present in the power delay profile for various threshold levels of -10 dB, -20 dB and -30 dB with respect to the maximum amplitude for (a) BS1 (Line of Sight scenario) and (B) BS4 (Non-Line of Sight scenario).

TABLE I.

LIMB MOVEMENT: NUMBER OF MULTIPATH COMPONENTS

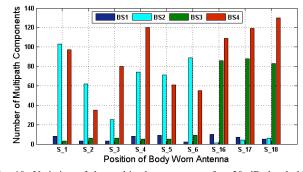|	BS Position	Threshold PDP		
		-10 dB	-20 dB	-30 dB
Sideways	**BS1,3**	**0-2**	**10-30**	**40-60**
	BS2	**0-2**	**10-40**	**75-125**
Forward	**BS1,2**	**0-2**	**10-25**	**50-75**
	BS3	**1-3**	**10-30**	**70-85**
Leg	**BS1,3**	**1-6**	**6-10**	**20-30**
	BS2	**5-10**	**60-80**	**150-175**
All Activities	**BS4**	**15-30**	**50-150**	**200-250**

Fig. 10. Variation of the multipath components for -20 dB threshold with respect to the base stations (BS1-BS4) and the wearable antenna. Antenna Positions S1-S3; S4-S6; S16-S18 (Right arm, Right leg, Torso centre).

Human Body Localisation: Figure 10 shows an example of the MPC's for different locations on the body for -20 dB threshold level. As observed in Fig. 10 and also in Table II., for the torso region, BS1 and BS2 have lower MPCs as LOS links are formed. For BS3 and BS4 NLOS links are formed as the body is obstructing the path leading to more multipath components.

As seen in Table II, maximum multipath are for the BS4 link for all the three thresholds considered. As observed from Table II., for left/right limbs BS2,4/BS1,3 links are in LOS scenario with lower range of MPCs in comparison to BS1,3/BS2,4 links which are generally in NLOS situation.

TABLE II.
WHOLE BODY: NUMBER OF MULTIPATH COMPONENTS

	BS Position	Threshold PDP		
		-10 dB	-20 dB	-30 dB
L limbs	BS1,3	7-10	60-75	165-175
	BS2,4	0-1	7-8	30-40
R limbs	BS1,3	0-2	5-6	25-40
	BS2	1-5	50-100	150-195
	BS4	5-10	50-100	150-200
Torso	BS1,2	1-6	6-10	20-30
	BS3	5-10	60-80	150-175
	BS4	20-25	100-120	200-250

Overall it is observed that -20/-30 dB threshold can easily distinguish between LOS and NLOS links. For -20 dB threshold of the power delay profile MPC below 10 can be considered as LOS link and MPC's above 30 indicate a NLOS link.

D. RMS Delay Spread

Limbs Localisation: Low RMS delay spread values in the range of 0.5 to 3 nsec are obtained for BS1 when the arm is moved sideways for 0° to 75° orientation and the values increase up to 9 nsec for 90° to 120°. For BS2, higher RMS delay spread values are obtained for arm motion (0° to 45°) and leg motion as the body-worn antenna is not in direct line of sight. Lower values of RMS delay spread are obtained for arm positions 90° to 120° as the antenna is clearly in direct line of sight with BS2,3 and the distance between the antenna and BS also reduces as the arm moves in the upward direction. Highest RMS delay values are obtained for the antennas placed on the leg with values reaching up to 20 nsec clearly demonstrating dense multipath and NLOS links between the antenna and BS4.
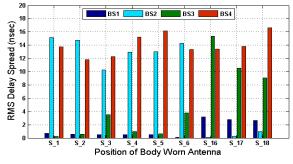

Fig. 11. Variation of the RMS delay spread of the received signal with respect to the base stations (BS1-BS4) and the wearable antenna. Antenna positions: S1-S3; S4-S6; S16-S18 (Right arm, Right leg, Torso centre).

Human Body Localisation: For the whole body localisation measurements, higher RMS delay spread (Fig. 11) is observed for the torso as both BS3 and BS4 (12 to 17 nsec) at the back are in NLOS situation causing interference and high multipath scenarios. Generally lower RMS spread values in the range of 0.1 to 5 nsec (75 % of the total values) are observed as BS1,2 are in direct line of sight situation with the wearable antennas. Considering BS3 for the right limbs, the trend observed is the increase in RMS delay spread from the antenna placed on the

shoulder to the antenna placed on the wrist as there is increase in the distance between the wearable node and BS. Hence, it can be seen that RMS delay spread is a good indicator to characterise the channel and classify the MS-BS links.

E. Kurtosis

Limbs Localisation: The Kurtosis values are in the range of 45 to 60 for BS1,2,3 showing higher probability of direct path and low multipath situation between the antenna and BS. For BS4, most of the antennas locations are in NLOS with the receiver, hence low Kurtosis index values (8-20) are observed. Highest values are observed for antennas placed on the wrist with respect to BS1 during sideways movements. Lowest Kurtosis values are observed for the legs especially for the thigh region, as maximum shadowing from the human body occurs for this region as BS4 is placed behind the subject.
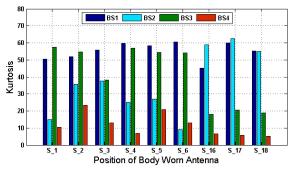

Fig. 12. Variation of the Kurtosis of the received signal with respect to the base stations (BS1-BS4) and the wearable antenna. Antenna positions: S1-S3; S4-S6; S16-S18 (Right arm, Right leg, Torso centre).

Human Body Localisation: Kurtosis index values in the range of 5 to 25 are observed for the antennas placed on the torso for BS3,4 as observed in Fig. 12. The highest Kurtosis values are observed for the base stations facing the limbs, e.g. for antennas placed on the right/left limb BS1,3/BS2,4 show higher Kurtosis index values. The thigh region shows low index values for BS4 and BS3 as these are mainly directed towards the back of the human subject. Very high Kurtosis index values (45 to 65) are observed for BS1 and BS3 for antennas (S1-S6) and for antennas (S7-S12) BS2 and BS4 show high Kurtosis values, the magnitude of the values vary depending upon the location of the antenna with respect to the BS. Results and analysis show that Kurtosis parameter is quite suitable to classify the radio channel and identify partial NLOS scenarios.

V.   LOCALISATION ACCURACY ANALYSIS

A. Localisation Results for Various Activities

High centimetre range accuracy is obtained using time of arrival UWB localisation techniques. The localisation accuracy depends on various factors such as base station configuration, propagation environment, signal to noise ratio, presence of objects and obstacles specifically dynamic ones such as the human body, location of the antennas with respect to the base station, accuracy of the localisation algorithm and sampling precision of the received impulse responses of IR UWB system.

The captured and analysed location estimation results are compared with the results obtained by a standard optical motion capture system, which is used as a reference. The results obtained for tracking of limb movement are listed in Table III

with 0.8 to 1.3 cm standard deviation and illustrated in Fig. 13 and Fig. 14. Various positions taken by the arms and legs are depicted in Fig. 15 and Fig. 16 respectively along with the tracking results obtained by the approach proposed. The average displacement error between subsequent limb motion captures is around 1 to 2 cm with standard deviation in the range of 0.9 to 1.4 cm. The detailed results obtained for the 3D displacement error (x, y and z) of the human body during limb movement activities is listed in Table IV. The results obtained show high accuracy in capturing the position of the limbs showing the suitability of the UWB technology for localisation and tracking.

Results for the localisation of the body worn antennas for the whole body localisation are shown in Fig. 17. The detailed results obtained for different locations of the human body are listed in Table V with a standard deviation of 0.7 to 1.3 cm. 3D localisation error obtained is in the range of 0.5 to 2.5 cm for overall positioning of the body worn antennas. Localisation accuracy results are best for the antennas placed on the arm in comparison to antennas placed on the legs as units placed on the legs incur more NLOS situations due to greater diameter than that of the arms. The average localisation accuracy for directional azimuth and elevation angles with respect to BS1 is approximately 1 to 2 degrees.
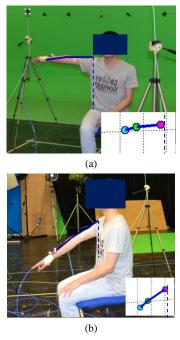

(a)

(b)

Fig. 13. Motion capture of UWB localisation for arm movement (a) 90° (sideways motion), (b) 60° (front motion). Inset: Pictorial representation of localisation of body worn antennas on the arm using UWB technology.
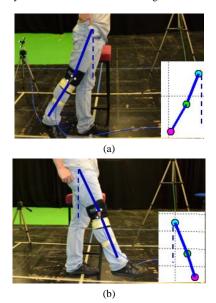

(a)

(b)

Fig. 14. Motion capture of UWB localisation for leg movement (a) -30° (backward motion), (b) 30° (forward motion). Inset: Pictorial representation of localisation of body worn antennas on the leg using UWB technology.
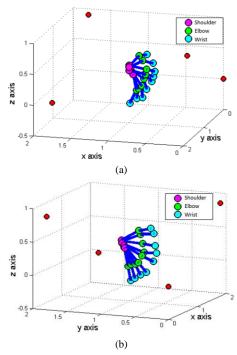

(a)

(b)

Fig. 15. UWB Arm Motion Localisation. (a) Sideways (b) Forward. Pink (shoulder), Green (Elbow), Blue (Wrist). All dimensions are in meters.
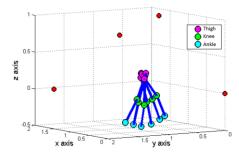

Fig. 16. UWB Leg Motion Localisation: Blue (Thigh), Green (Knee), Pink (Ankle). All dimensions are in metres.

The Geometric Dilution of Precision (GDOP) which shows the effectiveness of the placement of the BSs is computed for the BS configuration used with results in the range of 1-3 (2.15) stating very high positioning accuracy. Horizontal Dilution of Precision (HDOP) values and Vertical Dilution of Precision (VDOP) values for the BS configurations is 1.27 and 1.60 respectively [16]. Base station configuration selection has also been studied considering various random BS placement and comparing the performance with the configuration used.

This article has been accepted for publication in a future issue of this journal, but has not been fully edited. Content may change prior to final publication. Citation information: DOI 10.1109/TAP.2017.2759841, IEEE Transactions on Antennas and Propagation

> REPLACE THIS LINE WITH YOUR PAPER IDENTIFICATION NUMBER (DOUBLE-CLICK HERE TO EDIT) <　　　9

Results indicate that random BS configuration with occurrence of DOP values (5-10) can have a decrease in localisation accuracy by (1-2 cm) and that having very high GDOP values (>20) lead to decrease in accuracy by 3-5 cm.
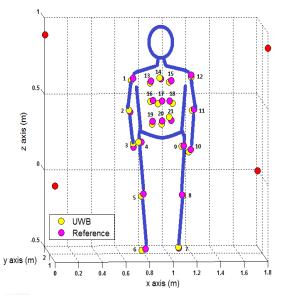

Fig. 17. Pictorial representation of body worn antenna localisation of comparing UWB based estimated positions with the reference actual positions

TABLE III.
LIMB MOVEMENT ACTIVITY - 3D LOCALISATION ACCURACY

Antenna Position	Average Localisation Error (cm)		
	X axis	Y axis	Z axis
Activity I: Arm Sideways Movement			
Shoulder	2.13	2.74	2.66
Elbow	2.07	1.60	1.86
Wrist	1.69	1.64	2.37
Activity II: Arm Forward Movement			
Shoulder	1.54	2.30	2.50
Elbow	1.48	1.31	1.57
Wrist	1.73	2.27	2.41
Activity III: Leg Forward and Backward Movement			
Thigh	2.25	2.03	2.50
Knee	1.59	1.47	2.10
Ankle	1.40	2.30	2.09

TABLE IV.
LIMB MOVEMENT ACTIVITY: 3D DISPLACEMENT ACCURCY

Activity	Average Displacement Error (cm)		
	X axis	Y axis	Z axis
Sideways Arm	1.41	2.21	2.05
Forward Arm	2.09	1.37	1.57
Forward and Backward Leg	1.30	1.89	2.02

Localisation accuracy depending on number of BS has also been explored leading to the conclusion that 8 BS can give slightly better accuracy in comparison to 4 BS but can increase the installation complexity, cost and time. Three BS will be able to provide 2D localisation and if used in L shape configuration

[23] can obtain 3D localisation with some deterioration in the accuracy (1 to 2 cm). Two BSs will not be able to give 2D or 3D localisation as it will be a limitation for the trilateration algorithm.

TABLE V.
WHOLE BODY: 3D LOCALISATION ACCURACY

Antenna Position	Average Localisation Error (cm)		
	X axis	Y axis	Z axis
Arms	1.21	1.16	1.5
Legs	1.40	1.67	1.07
Torso	1.74	1.89	1.91

B. Pulse Fidelity

The fidelity calculated shows good performance for different limb motion activities undertaken and overall body localisation by the TSA antennas, in preserving the shape of the received pulse at various angular orientations [24,42]. Fidelity factor is calculated between the transmitted and received signal using a sine modulated UWB pulse as source pulse. Table VI. summarises the fidelity values obtained and percentage of occurrence of these values for each BS.

TABLE VI.
FIDELITY ANALYSIS

		Fidelity Values			
		>0.95	0.95-0.85	0.85-0.8	0.8-0.7
Upper Limb	BS1,2,3	90 %	10 %		
	BS4	30 %	40 %	20 %	10 %
Lower Limb	BS1,2,3	90 %	10 %		
	BS4	30 %	50 %	15 %	5 %
Whole Body	BS1,2	80 %	20 %		
	BS3,4	50 %	30 %	10 %	10 %

For the arm motion (sideways and forward) very high fidelity results are observed for BS1,2,3 and for BS4 which generally incurs NLOS situations, there is more variation in fidelity with few values in the 0.70-0.80 range. In case of the right leg motion, for BS1,2,3; 90 % of the values are in the range of 0.95 and for the BS4 (NLOS scenario) 80 % of the values have fidelity factor greater than 0.85. Regarding the fidelity analysis of the whole body localisation, BS1,2 are having 80% fidelity values above 0.95 as the BSs form maximum LOS links with the werable antennas. For BS3,4 50 % values are above 0.95 as the occurrence of NLOS link is much higher. The complete fidelity analysis concludes that most of the measurements give a fidelity above 0.9. The high fidelity values makes TSA antenna as a potential candidate for body-centric wireless networks for localisation and tracking purposes.

VI. CONCLUSION

Accurate 3D limb movement tracking and whole body localisation has been obtained using compact, and cost-effective body-worn antennas in an indoor environment. High accuracy is obtained in the centimetre range (1 to 3 cm) suitable for human motion tracking, patient monitoring, physical rehabilitation and motion-capture applications. Average localisation accuracy as small as 0.5-2.5 cm has been achieved for 90 % of the scenarios, which is comparable to common commercial optical systems. Simple and robust localisation

scheme has been proposed for motion tracking and localisation applications taking into account NLOS mitigation and identification techniques. In-depth analysis of various wireless channel parameters has been carried out such as path loss magnitude, number of multipath components, received signal amplitude, RMS delay spread and Kurtosis. The work carried out gives an insight into propagation characteristics when antennas are placed on various body locations and the factors affecting the accuracy achieved while localising/tracking the antennas worn by the user in a potential wireless body sensor networks setup within body/personal area networks. The use of Kalman filter to improve tracking performance will be considered as possible future work for the body centric tracking and localisation research. Further experimental investigations and analysis will be undertaken by using a compact UWB transceiver chipset for body worn sensor localisation considering more dynamic movements and application specific environments to be deployed in real life healthcare applications.

REFERENCES

[1] A. R. Guraliuc, P. Barsocchi, F. Potortì and P. Nepa, "Limb Movements Classification Using Wearable Wireless Transceivers," *IEEE Transactions on Information Technology in Biomedicine,* vol.15, no.3, pp.474,480, May 2011.

[2] J. Andreu-Perez, D. R. Leff, H. M. D. Ip and G. Z. Yang, "From Wearable Sensors to Smart Implants-–Toward Pervasive and Personalized Healthcare," in *IEEE Transactions on Biomedical Engineering*, vol. 62, no. 12, pp. 2750-2762, Dec. 2015.

[3] M. D'Souza, T. Wark and M. Ros,, "Wireless localisation network for patient tracking," *International Conference on Intelligent Sensors, Sensor Networks and Information Processing, 2008. ISSNIP 2008.*, pp.79,84, 15-18 Dec. 2008.

[4] R. Cavallari, F. Martelli, R. Rosini, C. Buratti and R. Verdone, "A survey on wireless body area networks: Technologies and design challenges," *IEEE Communications Surveys Tutorials*, vol. 16, no. 3, pp. 1635–1657, 2014.

[5] D. Zhang, F. Xia, Z. Yang, L. Yao, and W. Zhao, "Localization technologies for indoor human tracking," in: *Proceedings of the IEEE International Conference on Future Information Technology(FutureTech'10)*, Pusan, Korea, May 2010.

[6] N. Bulusu, J. Heidemann and D. Estrin, "GPS-less low-cost outdoor localization for very small devices," in *IEEE Personal Communications*, vol. 7, no. 5, pp. 28-34, Oct 2000.

[7] Nissanka B. Priyantha, Anit Chakraborty, and Hari Balakrishnan. The cricket location-support system. In Proceedings of MOBICOM 2000, pages 32-43, Boston, MA, August 2000. ACM, ACM Press.

[8] S. Holm, "Hybrid ultrasound-RFID indoor positioning: Combining the best of both worlds," *2009 IEEE International Conference on RFID*, Orlando, FL, 2009, pp. 155-162.

[9] T. Liu, Y. Inoue, K. Shibata and R. Zheng, "Measurement of human lower limb orientations and ground reaction forces using wearable sensor systems," *2007 IEEE/ASME international conference on advanced intelligent mechatronics*, pp.1,6, 4-7 Sept. 2007.

[10] A. Guizar, C. Goursaud and J. M. Gorce, "Modeling the impact of node speed on the ranging estimation with UWB body area networks,"*2015 IEEE 26th Annual International Symposium on Personal, Indoor, and Mobile Radio Communications (PIMRC)*, 2015, pp. 1250-1254.

[11] Z. W. Mekonnen, E. Slottke, H. Luecken, C. Steiner and A. Wittneben, "Constrained Maximum Likelihood Positioning for UWB Based Human Motion Tracking,"*International Conference on Indoor Positioning and Indoor Navigation*, IPIN 2010, Zurich, Switzerland, pp. 1-10, Sept. 2010.

[12] M. R. Mahfouz, C. Zhang, B. C. Merkl, M. J. Kuhn and A. E. Fathy, "Investigation of High-Accuracy Indoor 3-D Positioning Using UWB Technology," *IEEE Transactions on Microwave Theory and Techniques*, vol.56, no.6, pp.1316,1330, June 2008.

[13] Xsens Motion Grid http://www.xsens.com/en/general/motiongrid

[14] A. J. Ali, W. G. Scanlon and S. L. Cotton, "Pedestrian effects in indoor UWB off-body communication channels," *Antennas and Popagation Conference (LAPC), 2010 Loughborough*, pp.57,60, 8-9 Nov. 2010.

[15] Clarke and A. Park, "Active-RFID system accuracy and its implications for clinical applications, *IEEE Symp. Computer-Based Med. Sys.*, Salt Lake City, USA, 2006, pp. 21-22.

[16] R. Bharadwaj, S. Swaisaenyakorn, C. G. Parini, J. Batchelor and A. Alomainy, "Localization of Wearable Ultrawideband Antennas for Motion Capture Applications," *IEEE Antennas and Wireless Propagation Letters*, vol.13, pp.507,510, 2014.

[17] R. Bharadwaj, C. Parini and A. Alomainy, "Experimental Investigation of 3D Human Body Localisation Using Wearable Ultra Wideband Antennas," *IEEE Transactions on Antennas and Propagation*, vol.63, no.11, pp.5035-5044, Nov. 2015.

[18] J. Hamie, B. Denis and M. Maman, "On-body localization experiments using real IR-UWB devices," *2014 IEEE International Conference on Ultra-WideBand (ICUWB)*, Paris, 2014, pp. 362-367.

[19] J. He, Y. Geng and K. Pahlavan, "Toward Accurate Human Tracking: Modeling Time-of-Arrival for Wireless Wearable Sensors in Multipath Environment," in *IEEE Sensors Journal*, vol. 14, no. 11, pp. 3996-4006, Nov. 2014.

[20] J. Corrales, F. Candelas, and F. Torres, "Hybrid tracking of human operators using IMU/UWB data fusion by a kalman filter," in *Proc. 3rd ACM/IEEE Int. Conf. Human Robot Interact. (HRI 2008)*, New York, NY, USA: ACM, pp. 193–200.

[21] H. A. Shaban, M. A. El-Nasr and R. M. Buehrer, "Toward a Highly Accurate Ambulatory System for Clinical Gait Analysis via UWB Radios," in *IEEE Transactions on Information Technology in Biomedicine*, vol. 14, no. 2, pp. 284-291, March 2010.

[22] S. Swaisaenyakorn, S. W. Kelly and J. C. Batchelor, "A Study of Factors Affecting Wrist Channel Characteristics for Walking Postures Using Motion Capture," *IEEE Transactions on Antennas and Propagation*, vol.62, no.4, pp.2231,2237, April 2014.

[23] R. Bharadwaj, C. Parini and A. Alomainy,"Ultra wideband-Based 3-D Localization Using Compact Base-Station Configurations," *IEEE Antennas and Wireless Propagation Letters*,vol.13, pp.221,224. 2014.

[24] A. Alomainy, A. Sani, A. Rahman, J. G. Santas and Y. Hao, "Transient Characteristics of Wearable Antennas and Radio Propagation Channels for Ultrawideband Body-Centric Wireless Communications,"*IEEE Transactions on Antennas and Propagation*, vol.57, no.4, pp875-884, April 2009.

[25] 2014.I. Guvenc, C. C. Chong and F. Watanabe, "Joint TOA Estimation and Localization Technique for UWB Sensor NetworkApplications," *Vehicular Technology Conference, 2007. VTC2007-Spring. IEEE 65th*, pp.1574,1578, 22-25 April 2007.

[26] D. Dardari, A. Conti, U. Ferner, A. Giorgetti and M. Z. Win , "Ranging With Ultrawide Bandwidth Signals in Multipath Environments," *Proceedings of the IEEE* , vol.97, no.2, pp.404,426, Feb. 2009.

[27] D. Humphrey and M. Hedley, "Prior Models for Indoor Super-Resolution Time of Arrival Estimation,"*Vehicular Technology Conference, 2009. VTC Spring 2009. IEEE 69th*, pp.1-5, 26-29 April 2009.

[28] I. Guvenc, C. C. Chong and F. Watanabe, "NLOS Identification and Mitigation for UWB Localization Systems," *2007 IEEE Wireless Communications and Networking Conference*, Kowloon, 2007, pp. 1571-1576.

[29] B. Denis, J. Keignart and N. Daniele "Impact of NLOS propagation upon ranging precision in UWB systems," *2003 IEEE Conference on Ultra Wideband Systems and Technologies*, pp.379,383, 16-19 Nov. 2003.

[30] I. Guvenc and Z. Sahinoglu, "Threshold selection for UWB TOA estimation based on kurtosis analysis", *IEEE Commun. Lett.*, vol. 9, pp. 1025-1027, Dec. 2005.

[31] J. Schroeder, S. Galler, K. Kyamakya and K. Jobmann, "NLOS detection algorithms for Ultra-Wideband localization," *Positioning, Navigation and*

*Communication, 2007. 4th Workshop on WPNC '07,*pp.159,166, 22-22 March 2007.

[32] S. Marano, W. M. Gifford, H. Wymeersch and M. Z. Win, "NLOS identification and mitigation for localization based on UWB experimental data," *IEEE Journal on Selected Areas in Communications*, vol.28, no.7, pp.1026,1035, September 2010.

[33] I. Guvenc and C. C. Chong, "A Survey on TOA Based Wireless Localization and NLOS Mitigation Techniques," *IEEE Communications Surveys & Tutorials,* vol.11, no.3, pp.107,124, 3rd Quarter 2009.

[34] I. Guvenc and Z. Sahinoglu, "Threshold-based TOA estimation for impulse radio UWB systems," *IEEE International Conference on Ultra-Wideband, 2005. ICU 2005. 2005* pp.420,425, 5-8 Sept. 2005.

[35] M. J. Kuhn, J. Turnmire, M. R. Mahfouz and A. E. Fathy, "Adaptive leading-edge detection in UWB indoor localization," *2010 IEEE Radio and Wireless Symposium (RWS)*, pp.268,271, 10-14 Jan. 2010.

[36] Z. Sahinoglu, S. Gezici, and I. Guvenc, Ultra-wideband positioning systems:theoretical limits, ranging algorithms, and protocols. Cambridge Univ Press,2008.

[37] A. H. Sayed, A. Tarighat and N. Khajehnouri, "Network-based wireless location: challenges faced in developing techniques for accurate wireless location information,"*IEEE Signal Processing Magazine*, vol.22, no.4, pp. 24- 40, July 2005.

[38] K. W. Cheung, H. C. So, W. K. Ma and Y. T. Chan, "Least squares algorithms for time-of-arrival-based mobile location,"*IEEE Transactions on Signal Processing*, vol.52, no.4, pp.1121,1130, April 2004.

[39] S. Ghassemzadeh and V. Tarokh, "A statistical path loss model for in-home UWB channels," *IEEE Conference on Ultra Wideband Systems and Technologies*, pp. 59–64, May 2002.

[40] A. Fort, C. Desset, J. Ryckaert, P. De Doncker, L. Van Biesen and S. Donnay, "Ultra wideband body area channel model," *International Conference on Communications, ICC05, Seoul, South Korea*, May 2005.

[41] A. Fort, C. Desset, P. De Doncker, P. Wambacq and L. Van Biesen, "Ultra wideband body area propagation:from statistics to implementation," *IEEE Transactions on Microwave Theory and Technique*, vol. 54, no. 4, pp. 1820–1826, June 2006.

[42] R. Bharadwaj, C. Parini and A. Alomainy, "Analytical and Experimental Investigations on Ultrawideband Pulse Width and Shape Effect on the Accuracy of 3-D Localization," in *IEEE Antennas and Wireless Propagation Letters*, vol. 15, no. , pp. 1116-1119, 2016.